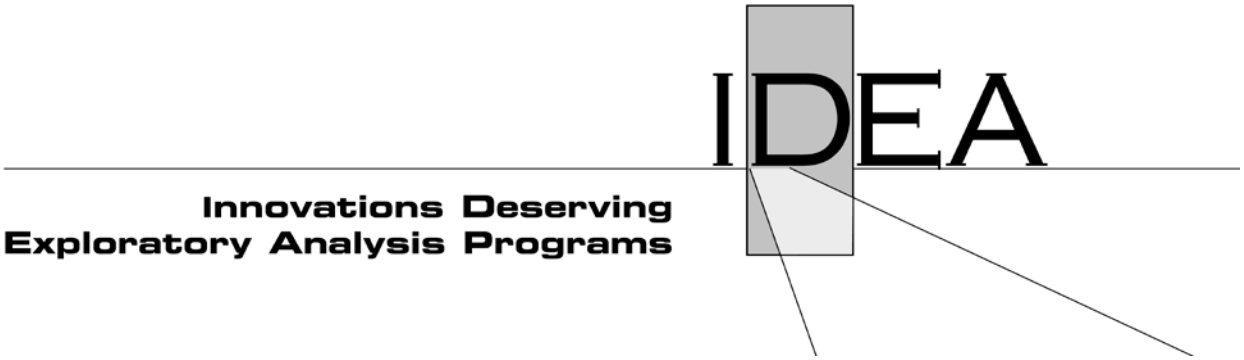

Rail Safety IDEA Program

ADAPTIVE PRESTRESSING SYSTEM FOR CONCRETE CROSSTIES

Final Report for
Rail Safety IDEA Project 33

Prepared by:
Bassem Andrawes
University of Illinois at Urbana-Champaign

November 2019

TRB TRANSPORTATION RESEARCH BOARD
The National Academies of
SCIENCES · ENGINEERING · MEDICINE

Innovations Deserving Exploratory Analysis (IDEA) Programs Managed by the Transportation Research Board

This IDEA project was funded by the Rail Safety IDEA Program.

The TRB currently manages the following three IDEA programs:

- The NCHRP IDEA Program, which focuses on advances in the design, construction, and maintenance of highway systems, is funded by American Association of State Highway and Transportation Officials (AASHTO) as part of the National Cooperative Highway Research Program (NCHRP).
- The Rail Safety IDEA Program currently focuses on innovative approaches for improving railroad safety or performance. The program is currently funded by the Federal Railroad Administration (FRA). The program was previously jointly funded by the Federal Motor Carrier Safety Administration (FMCSA) and the FRA.
- The Transit IDEA Program, which supports development and testing of innovative concepts and methods for advancing transit practice, is funded by the Federal Transit Administration (FTA) as part of the Transit Cooperative Research Program (TCRP).

Management of the three IDEA programs is coordinated to promote the development and testing of innovative concepts, methods, and technologies.

For information on the IDEA programs, check the IDEA website (www.trb.org/idea). For questions, contact the IDEA programs office by telephone at (202) 334-3310.

IDEA Programs
Transportation Research Board
500 Fifth Street, NW
Washington, DC 20001

ADAPTIVE PRESTRESSING SYSTEM FOR CONCRETE CROSSTIES

IDEA Program Final Report

Rail Safety IDEA Project 33

Prepared for the IDEA Program
Transportation Research Board
The National Academies

Bassem Andrawes
Department of Civil and Environmental Engineering
University of Illinois at Urbana-Champaign

November 15, 2019

ACKNOWLEDGEMENTS

The author would like to thank the Transportation Research Board (TRB) and the Rail Safety (RS) IDEA program for funding this project. Special thanks to RS program manager, Dr. Velvet Basemera-Fitzpatrick and External Review Panel members, Mr. John Bosshart, Mr. David Davis, and Mr. Conrad Ruppert for their invaluable advice and comments during the project.

TABLE OF CONTENTS

LIST OF FIGURES

LIST OF TABLES

EXECUTIVE SUMMARY

This IDEA project focused on developing an Adaptive Prestressing System (APS) for concrete crossties. The new prestressing system utilizes a unique characteristic of a class of smart materials known as Shape Memory Alloys (SMAs). Through heating, a SMA can recover its original shape after being excessively deformed beyond its elastic range. This shape memory phenomenon of SMAs can be used as a mean for prestressing concrete by embedding prestrained SMA wires in the concrete. When heated, the SMA will attempt to shrink inducing large recovery stress within the SMA that will in turn transfer to the surrounding concrete in the form of prestressing force. NiTiNb SMA were used in this study to prestress concrete crossties in the form of APS. APS can be described as a fuse made of SMA wires connected to steel wires in series. The APS is utilized to apply prestress only at target regions in the crosstie.

The research work comprised three main phases: (1) validating local prestressing using SMA wires only, (2) developing the APS, and (3) structural testing of concrete crossties using APS. First, to validate the use of SMA as prestressing material in concrete, 2mm diameter NiTiNb SMA wires were used as prestressing reinforcement in small-scale 30 in. long concrete crosstie specimens. The prestressing system comprised two SMA wires bundled together and wrapped with nylon sleeves for debonding. The number of bundles and their eccentricities in the crosstie's rail seat and center regions were designed as per a reference AREMA-based tie. Three small scale concrete crosstie specimens were designed with different SMA prestressing system configurations, namely, straight, L-shaped, and U-shaped. Digital Image Correlation (DIC) and strain gauges were used to capture strain distribution within the ties during prestressing. The test results showed that SMA was able to apply prestressing force locally in the crossties at the intended locations.

The second phase of the project focused on the design and development of APS for crosstie prestressing. An APS consists of steel and SMA wires connected mechanically in series to act as a prestressing reinforcement in the tie. When the SMA wire in the APS (named fuse) is activated, i.e. heated, recovery stress generates in SMA transferring through the connection to the steel wires. In this application, SMA fuse is used as mechanism through which steel wires are easily stressed without the need for conventional hydraulic jacking/stressing. Testing was carried out to ensure that the connection between SMA and steel is able to hold the prestressing force within the system. A study was carried out to design the APS and determine the length and cross sectional area of both steel and SMA. Designed APS was then embedded in a prismatic concrete beam and tested for validation. The results illustrated the ability of the designed APS to prestress the beam at targeted regions.

The last phase of the project focused on testing a reduced-scale concrete crosstie prestressed with the new APS. Tested specimen was designed as ½ scale of the AREMA-based reference tie. Three and two APS assemblies were embedded in rail seat and center regions with 1.0 in. and 0.6 in. eccentricities, respectively. Activation of the APS (i.e. SMA heating) was followed by flexural testing of both rail seat and center regions. DIC and strain gauges were used to monitor the deformation in the crosstie during prestressing and under applied load. The heating of the SMA fuse was conducted using torch flames. The axial strain distribution from DIC matched closely the predictions from FE models, which proved that the prestress was applied to the targeted regions (bottom of rail seat and top of center section). In addition, the activation of APS in one region does not affect the strain distribution of the rest of the crosstie. Hence, APS can apply prestress only in a localized region as desired. After the application of prestress, four-point bending tests at rail seat and center sections were performed. The results showed that the cracking load closely matched the design cracking load. Due to the use of steel reinforcement at the compression zones, the post peak behavior was largely ductile with a gradual strength degradation. This phase of the project proved the success of the proposed APS in applying prestress to a targeted region in the crosstie.

1. IDEA PRODUCT

The product of this IDEA project is an Adaptive Prestressing System (APS) that can be used for prestressing concrete crossties. Unlike conventional prestressing methods (i.e. pre-tensioning or post-tensioning), APS can apply prestressing with varying levels at targeted regions using Shape Memory Alloy (SMA) wires. APS provides also flexibility in adjusting the level of prestress along the crosstie as needed. The proposed APS consists of SMA fuse (wire) connected in series with steel reinforcement using mechanical connections. The shape recovery feature of the SMA fuse is utilized to prestress the steel reinforcement without the need for external stressing or jacking devices. The elimination of mechanical jacking reduces a great deal of labor and time in addition to decoupling the processes of crosstie casting and prestressing. Adopting APS will facilitate casting of concrete ties in a regular mold instead of specially equipped cast beds that are needed for pre-tensioning of steel wires, which will help increase the production of crossties. In addition, APS can be activated at any age of concrete, which can reduce prestress losses associate with creep and shrinkage of concrete at early age; hence improve the quality of produced crossties. Furthermore, this research clearly proved the feasibility of the new APS to apply prestress to a specific region in the crosstie, which will help optimize the design of crossties making them more efficient.

2. CONCEPT AND INNOVATION

The concept of "***Adaptive Prestressing System (APS)***" is based on introducing, monitoring and adjusting prestress forces within the tie in the field. With the use of innovative prestressing materials, it is believed that a method can be developed to introduce prestress in specific areas of concrete as needed by embedding shape memory alloy (SMA) fuses in the required region(s). This could not be done in conventional prestressing methods (pretensioning or post-tensioning) which apply constant prestressing to the entire length of the crosstie to achieve the desired strength, resulting in an inefficient system. Further, in conventional methods, there is no simple way for adjusting the level of prestress once the stress has transferred to the concrete.

The proposed Adaptive Prestressing System (APS) incorporates short prestressing fuses made of shape memory alloys (SMAs). SMAs are a class of metallic alloys that exhibit unique capability of recovering their original (un-deformed) shape after being excessively deformed. The shape recovery could be attained by heating the alloy to a temperature above the transformation temperature, A_f, which is a fixed property of the alloy predetermined by the user/manufacturer. The idea of using SMAs in providing prestress for concrete is based on utilizing the recovery stress associated with the shape recovery (Shape Memory Effect) of the SMAs when heated. This recovery stress could reach up to 120 ksi depending on the material characteristics as well as on the level of deformation experienced prior to shape recovery (Otsuka and Wayman 2002[1]). Small segments called "*fuses*" made of SMAs are manufactured with a length much shorter than the actual length of the crosstie (approximately 5% – 10% of the tie's length). These SMA fuses will then be placed in series with the prestress wires at the desired locations before the concrete is cast (figure 1). Once the concrete has been placed and cured, the fuses will be ready to be heated to activate the prestress prior to installing the ties on track. The SMA fuse activation could be done using electrical resistivity either at the concrete plant before shipping the crossties or in the field (see enlarged image in figure 1). Once heating begins, the SMA fuses will attempt to shrink to their original length. This will develop a recovery stress (prestress) which will in turn develop an axial stress in the prestress wires/strands. Over the service life of the tie the prestressing force in the system can be monitored frequently through measuring the electrical resistivity of the SMA fuses, and if needed adjusted by passing an electrical current in the fuse without the need for taking the tie out of service (figure 1).

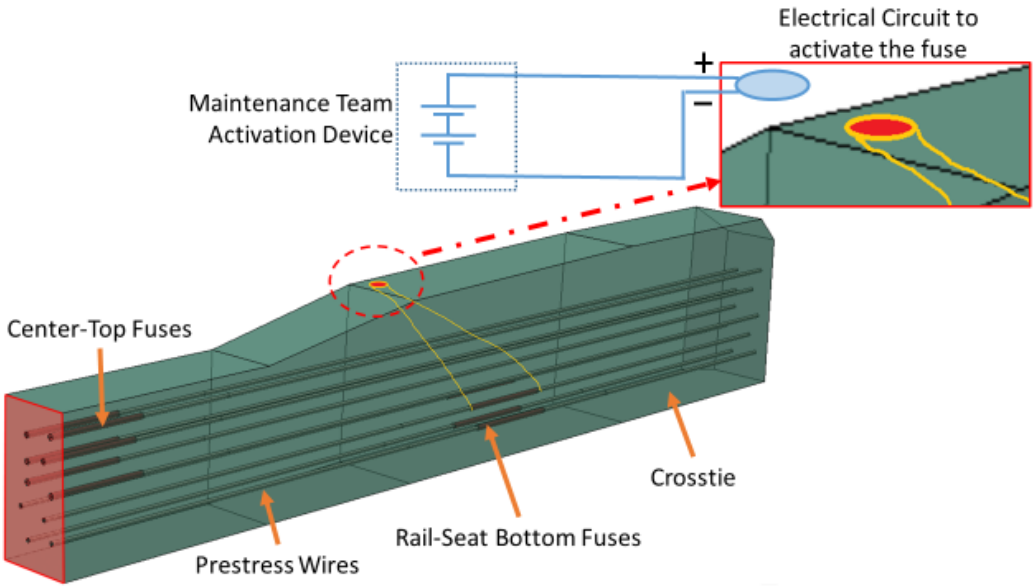

Figure 1 3D view of the embedded SMA fuses in series with the prestress wires/strands. Enlarged image shows a potential activation mechanism for the fuse using electrical circuit.

The proposed APS can be divided into three zones (regions) along the crossties (figure 2). Zone 1 is the region where unbonded SMA fuse is placed with its end connections to the steel prestressing wires. Zone 2 is the region where unbonded steel wire connected with SMA fuse is placed. Activating the fuse in Zone 1 will engage the steel in Zone 2. Zone 3 is an anchorage region where extended steel wire from zone 1 (figure 2a) or zone 2 (figure 2b) is bonded to concrete. By arranging these zones in APS, there can be more than one design for the APS. For example, two types of APS are schematically displayed in figures 2a and 2b. Figure 2a shows a case where only one side of SMA fuse (zone 1) is connected to the unbonded steel wire (zone 2) and the other end is anchored to concrete by a bonded steel wire (zone 3). However, figure 2b shows a case where both ends of SMA fuse (zone 1) are connected to unbonded steel wires (zone 2). In figure 2a and 2b, yellow gradient fill represents the applied prestress after the activation of APS (heating SMA fuse). It is shown that prestressing force is applied at zones 1 and 2. Either types of APS are applicable in concrete crossties. Especially, figure 2a can be adopted where target prestressing region is relatively short.

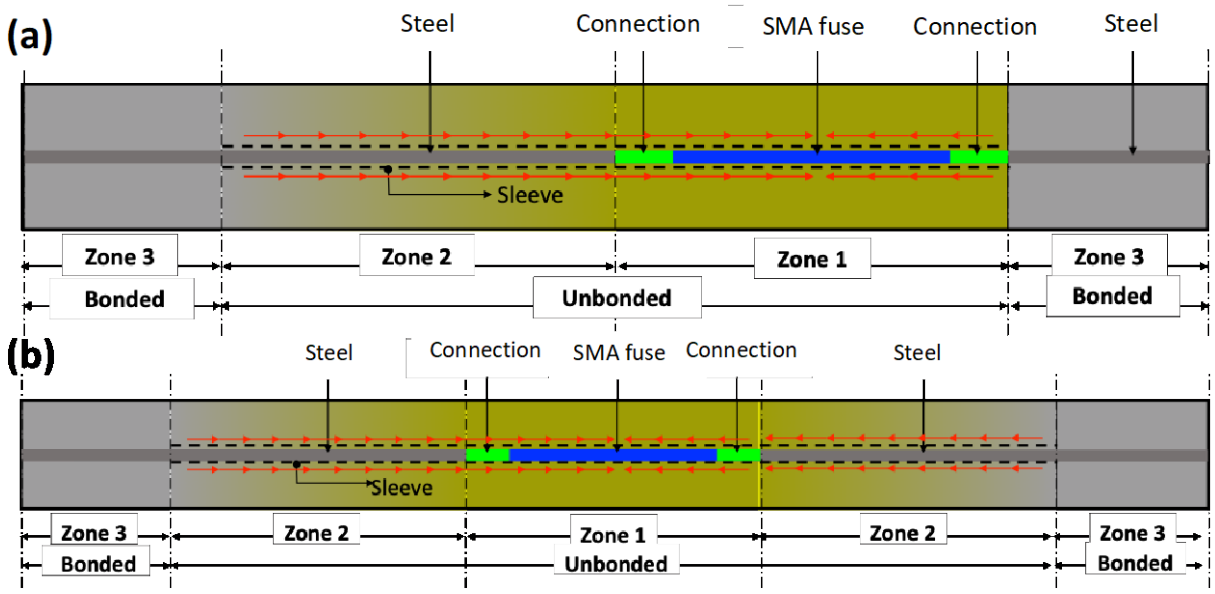

Figure 2 Schematics of two types of APS

There are multiple advantages for the proposed APS including:

- **Flexibility to prestress a specific area of the crosstie.** It is well known that the entire length of the crosstie has to be prestressed to provide sufficient strength for center-negative and rail-seat-positive moment capacities. By using the proposed SMA fuses, there is a flexibility to prestress a specific area along the length or depth of the crosstie. Therefore, instead of prestressing the entire length of the crosstie, center-top and rail-seat bottom can be independently prestressed by placing appropriate number of SMA fuses there.
- **Reduce prestress losses.** Ideally, SMA fuse should be activated when concrete reaches its target strength (e.g. at 28 days). The delay in prestressing the concrete will help significantly in reducing prestress losses due to concrete creep and shrinkage.
- **Ability to monitor and change the prestress level on the track without requiring to remove/replace the crosstie.** The stress in the SMA fuses can be monitored and controlled simply by electrical resistivity. As a result, the prestress level in the crosstie can be varied by maintenance teams without having to remove/replace the crosstie. The crosstie undergoes millions of load cycles and faces varied support conditions throughout its life, resulting in prestress variation. The ability to change the prestress level will help improve the performance and safety of the ties and avoid retiring them before their design life.
- **No external hydraulic jacking is required** in applying the prestressing force, which saves on the production costs of the crossties. The prestressing force is applied by heating the SMA fuses. This saves on the amount of hardware and labor required and thus will facilitate the application of the post-curing prestressing independent of concrete shrinkage and creep losses.
- **Studies have proven that SMAs are not affected by creep** at temperatures below 250^0C. This will lead to a reliable and maintained level of prestressing with time, i.e. there will be no losses in the prestressing fuses. A problem highly observed in steel.
- **The SMAs has proven to be highly resistant to corrosion**. This will eliminate any possibility of SMA fuse deterioration due to weather or surrounding environmental conditions and will require a much less level of maintenance for the installed fuses.
- **Concern regarding de-bonding between steel wires and concrete is reduced.** There is always a concern of losing part of the prestress force due to de-bonding of the steel wires after concrete cracks. In the case of the proposed APS, both the SMA fuse and steel wires are de-bonded intentionally in order to provide more uniform stress distribution in the surrounding concrete along the length of the crosstie.

3. INVESTIGATION

3.1. Small-scale local prestressing system using SMA wires

3.1.1. Specimen design

The geometry of the small-scale specimens used in the study was simplified and scaled down of the typical concrete crosstie. The length of the specimen was 30in, the width of the section was 3in throughout the length of the tie and the height of the section is 3in and 2.3in at rail seat and center region, respectively.

Nickel Titanium Niobium (NiTiNb) SMA wires with 2mm diameter were used in the study. The wires have a constrained recovery stress of 79.77 ksi and recovery force of 0.3884 kip per wire. This recovery stress can be achieved by heating the NiTiNb wires up to 200°C. The concrete mix was designed to a target compressive strength of 3 ksi in 28 days. The activation of the SMA wires was done in 3 days after casting. The concrete strength in 3 days was 2461.5 psi.

The section was designed to have some equivalency to the existing concrete crosstie design. The design goal was to achieve comparable amount of stress at the bottom of the critical section after prestressing. Two SMA wires were bundled and wrapped with nylon sleeves which act as a debonding duct to concrete and an insulator. In rail seat sections, 4 – (2) 2mm diameter NiTiNb wire bundles were placed at 0.5in from the bottom of the section with the spacing of 0.6in (figure 3a). In center sections, 3 – (2) 2mm diameter NiTiNb wire bundles were placed at 0.5in from

the top of the section with a spacing of 0.75in (figure 3a). The designed sections could achieve 77.06% and 51.72% of the bottom stress of the real rail ties at the rail seat and center sections, respectively.

One of the advantages of the APS is the freedom of wire arrangements throughout the length. In this study, three different wire arrangements were designed: Straight, L-shaped, and U-shaped wire arrangements in specimens SP1, SP2, and SP3, respectively (figure 3b). The diagonal component of L-shaped and U-shaped wires were designed to reinforce the ties in shear, because the rail seat region was prone to shear failure.

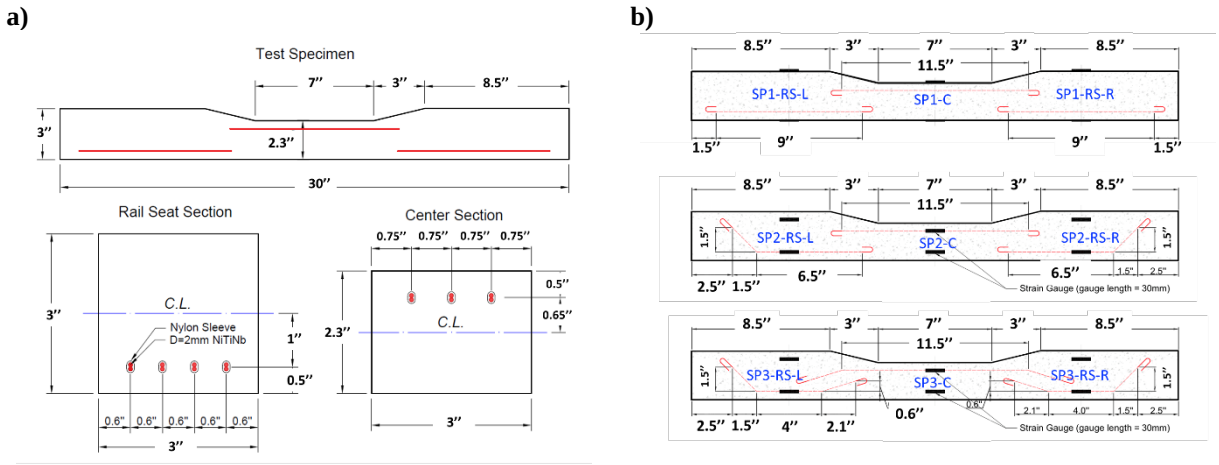

Figure 3 a) Specimen dimensions and section designs, b) Three different wire arrangements of the specimens

3.1.2. Test Setup

Strain distribution in the specimen was measured during and after the activation (heating) of the SMA wires. To measure the strain distribution at the surface of the specimen, the Digital Image Correlation (DIC) technique was used. As shown in figure 4, camera was placed in front of the specimen to capture frames during and after the activation of SMA wires. To verify the strain measured from DIC, strain gauges were attached to the top and bottom of the tie (figure 3b and 4). Due to the limited resolution of the DIC camera used, the SMA activation was performed separately on left rail seat, center, and right rail seat regions.

Electrical resistivity was used to heat the SMA wires. Copper lead wires were connected to both ends of the SMA wires to form a closed circuit with DC power supply (figure.4). Temperature of the wires was monitored during the heating of the SMA wires. A thermo-couple was placed in contact with the SMA wires, penetrating through the nylon sleeve which wraps the SMA wires (figure.4). The DC power supply was disconnected when the temperature reached 200°C to prevent the overheating which could possibly damage the concrete in early age.

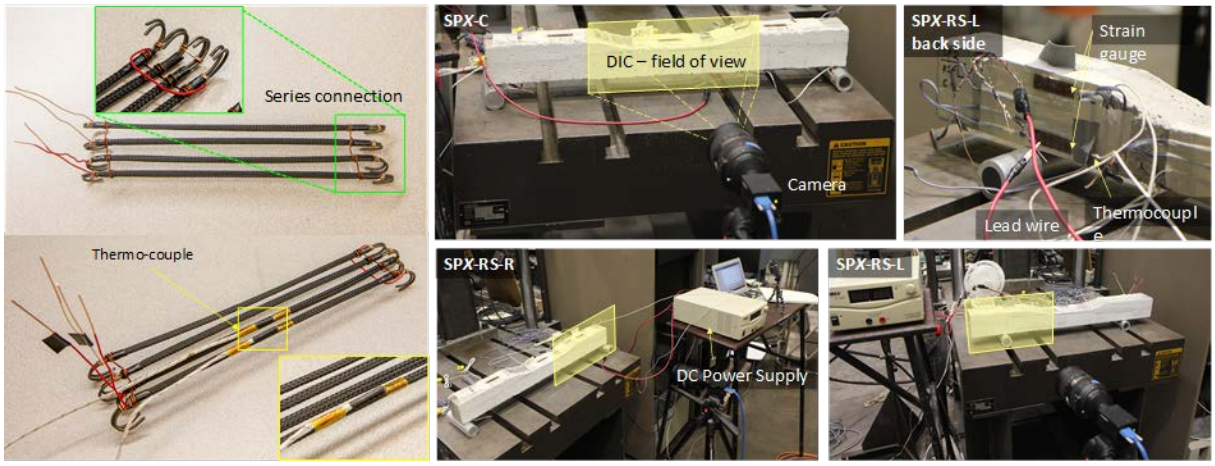

Figure 4 SMA wire assembly and test setup

3.1.3. Test Results

Figure 5 shows the temperature measured from the thermo-couple and strains measured from the strain gauges of the test at the center region of specimen SP1. It was shown that the strains at top and bottom increases in compression and tension respectively, as the temperature increases. There were two peaks in temperature curve, because the SMA wires were heated sequentially two wires at a time.

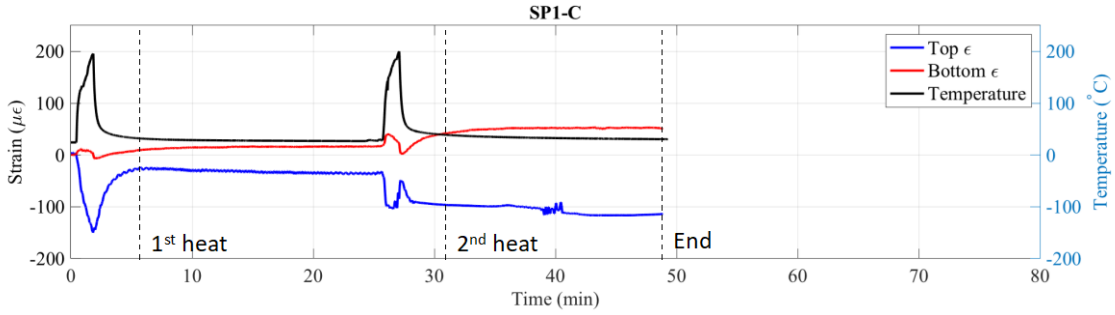

Figure 5 Time history of strains and temperature at SP1-C

Figure 6a, 6b, and 6c show the axial strain distributions of SP1, SP2, and SP3 measured by DIC and finite element analysis results. It was observed that the axial strain distributions from DIC and FEM were almost identical. Figure 7a and 7b show the shear strain distribution of SP2 and SP3, respectively. SP2 and SP3 have diagonal SMA wires which is designed to reinforce the ties in shear. It was shown that diagonal components were contributing to the shear stress at the rail seat region. As shown in figures 5, 6, and 7, the SMA wires embedded in concrete successfully applied the prestressing as designed.

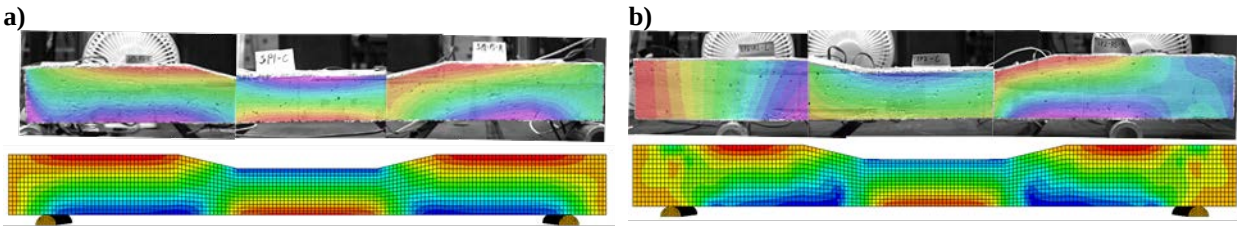

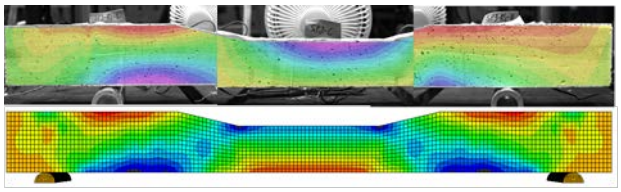

Figure 6 Comparison of DIC and FE model prediction of axial strains for a) SP1, b) SP2, and c) SP3

a) **b)**

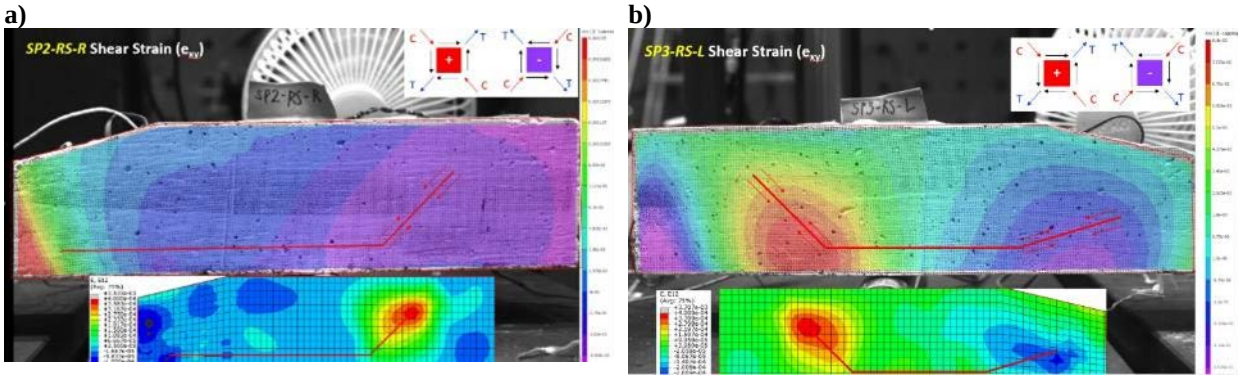

Figure 7 Comparison of DIC and FE model prediction of shear strain of a) SP2-RS-R, and b) SP3-RS-L

3.2. APS Development

3.2.1. Recovery stress of APS

To develop a relationship between the partial strain recovery and the corresponding recovery stress of SMA, the recovered strain values were plotted against the recovery stress as presented in Figure 8. It was observed that a linear relation exists between partial strain recovery and percent of σ_{rec} developed. The linear trend-line established the relationship which was used to predict the proportioning of the SMA fuse with respect to the steel wires.

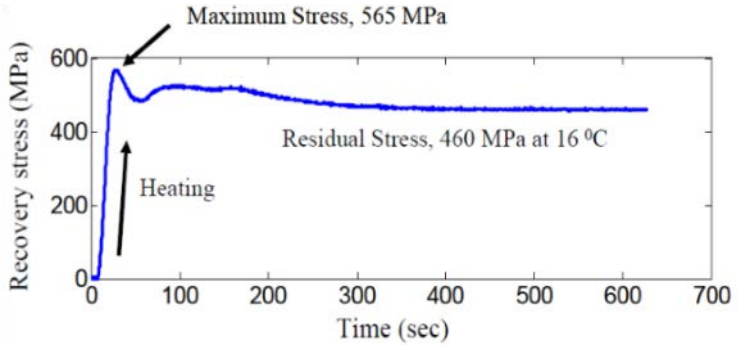

Figure 8 Recovery stress behavior adopted in the study for the SMA fuse (1ksi = 6.895 MPa)

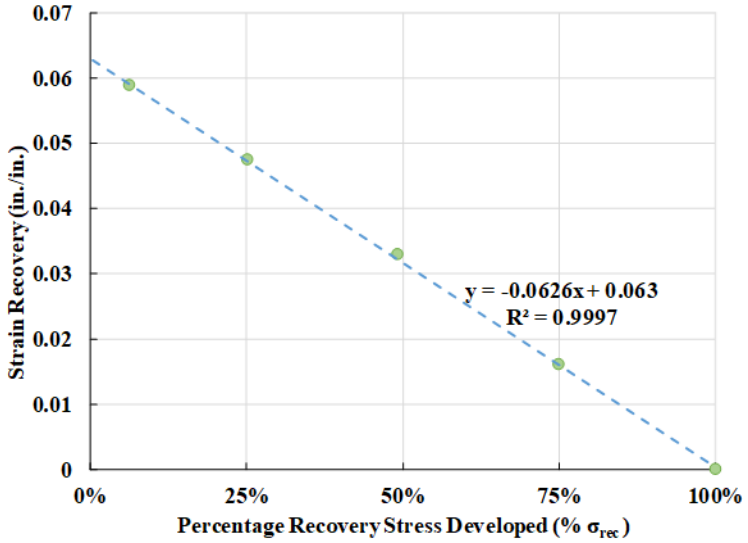

Figure 9 Developed relationship between SMA strain recovery and recovery stress

Having characterized the material properties, it was attempted to predict the recovery stress developed in the SMA-steel assembly depending upon the geometry of the two materials. The linear trend-line predicted in Figure 9 was used to develop a theoretical model and was represented by eqn. (1). Here σ_{rec} was the recovery stress corresponding to full restraint conditions, i.e. 79.77 ksi, and ϵ_{pre} was the prestrain in the SMA wire used, i.e. 6.3%. Using Hooke's law and force equilibrium equations, the final form of equation was obtained as eqn. (2). As the geometric and materialistic properties were known, the relation between recovery stress developed in the SMA fuse and the length ratio of steel wire and SMA fuse was established as shown in eqn. (3).

$$\epsilon_{rec} \approx 0.063 - 0.063\left(\frac{\sigma_{SMA}}{\sigma_{rec}}\right) = \epsilon_{pre} - \epsilon_{pre}\left(\frac{\sigma_{SMA}}{\sigma_{rec}}\right) \quad \text{--- (1)}$$

$$\sigma_{SMA} = \frac{\epsilon_{pre}}{\left(\frac{\epsilon_{pre}}{\sigma_{rec}}\right) + \frac{2}{E_{steel}}\left(\frac{A_{SMA}}{A_{steel}}\right)\left(\frac{L_{steel}}{L_{SMA}}\right)} \quad \text{--- (2)}$$

$$\sigma_{SMA} = \frac{913.5}{11.45 + \left(\frac{A_{SMA}}{A_{steel}}\right)\left(\frac{L_{steel}}{L_{SMA}}\right)} \quad (ksi) \quad \text{--- (3)}$$

Eq. (3) was used to conduct a parametric study to explore the effect of varying the volume (length and area) of SMA versus steel on the recovery stress developed in the assembly. A summary of the results is presented in tables 1 and 2. These tables were used to examine various scenarios of prestressing concrete blocks using APS.

Table 1 Recovery stress developed in SMA per volume ratio and length ratio (ksi)

Length Ratio $\left(\frac{L_{st}}{L_{SMA}}\right)$	Area Ratio $\left(\frac{A_{st}}{A_{SMA}}\right)$ 0.25	0.5	0.75	1	1.25	1.5	1.75	2	2.25	2.5
5	23.26	17.06	13.47	11.13	9.48	8.26	7.31	6.56	5.95	5.45
4.5	27.60	19.88	15.54	12.75	10.81	9.39	8.29	7.43	6.72	6.14
4	33.32	23.52	18.18	14.81	12.50	10.81	9.52	8.51	7.69	7.02
3.5	41.07	28.34	21.63	17.49	14.68	12.65	11.11	9.91	8.94	8.14
3	52.01	34.96	26.33	21.12	17.63	15.13	13.25	11.79	10.61	9.65
2.5	68.24	44.51	33.03	26.25	21.78	18.62	16.25	14.42	12.96	11.77
2	94.08	59.25	43.24	34.04	28.07	23.88	20.78	18.39	16.49	14.95
1.5	139.85	84.47	60.51	47.14	38.61	32.69	28.35	25.02	22.40	20.27
1	236.98	136.15	95.51	73.56	59.81	50.39	43.54	38.32	34.22	30.92
0.5	544.61	294.23	201.57	153.29	123.67	103.64	89.20	78.29	69.75	62.90

Table 2 Stress developed in steel per volume ratio and length ratio (ksi)

Length Ratio $\left(\frac{L_{st}}{L_{SMA}}\right)$	Area Ratio $\left(\frac{A_{st}}{A_{SMA}}\right)$ 0.25	0.5	0.75	1	1.25	1.5	1.75	2	2.25	2.5
5	116.30	85.30	67.35	55.64	47.40	41.28	36.57	32.82	29.76	27.23
4.5	124.21	89.48	69.92	57.39	48.66	42.24	37.31	33.42	30.26	27.64
4	133.27	94.08	72.71	59.25	49.99	43.24	38.09	34.04	30.77	28.07
3.5	143.75	99.19	75.72	61.23	51.40	44.28	38.90	34.68	31.29	28.51
3	156.03	104.89	78.99	63.36	52.88	45.38	39.75	35.36	31.84	28.96
2.5	170.60	111.28	82.56	65.63	54.46	46.54	40.63	36.05	32.40	29.42
2	188.17	118.49	86.47	68.08	56.13	47.76	41.56	36.78	32.99	29.90
1.5	209.77	126.71	90.77	70.71	57.91	49.04	42.52	37.53	33.59	30.40
1	236.98	136.15	95.51	73.56	59.81	50.39	43.54	38.32	34.22	30.92
0.5	272.31	147.12	100.78	76.64	61.83	51.82	44.60	39.14	34.88	31.45

3.2.2. APS connection mechanism

To make APS work properly, the development of a robust connection mechanism that could hold steel and SMA wires together when activated was essential. The optimal way of connecting steel and SMA wires would be welding to minimize the connection length, as well as to hold enough strength. However, in this proof-of-concept study, connection of SMA and steel was done to meet basic requirement, strength, just because the size of the SMA wire used in this study was only 2mm diameter. In future work, the connection mechanism of large diameter SMA wires and steel could be improved further.

In this study, multiple alternative connection mechanisms were examined to verify their strengths. Mechanical connections such as U clamps, crimped steel tubes, and split bolts, and high strength epoxy adhesive were explored. The list of alternative connection mechanisms is shown in the Table3. Each connection mechanism was designed to hold maximum number of SMA wires considering its geometric constraints. The target force of each connection mechanism was the total recovery force generated from SMA wires when activated. The uniaxial tensile tests of the APS using connection mechanisms listed in Table 3 were performed and the results are shown in Figure 10. None of the mechanical connections without high strength adhesive satisfied the target force. Only three connection mechanisms (Uclmp_3_Epx, Uclmp_2_EPx, and Split_2_Cut_1in_Epx) were able to surpass the target force.

Table 3 List of alternative connection mechanisms

Specimen	Max load (kip)	Target force (kip)	OK?	# of SMA	Connector	Connection length	Epoxy
Uclmp_3_Epx	5.23	3.11	Y	8	(3) 1/4" U clamp	2.0 in	o
Uclmp_2_Epx	3.51	3.11	Y	8	(2) 1/4" U clamp	1.5 in	o
Uclmp_3	1.15	3.11	N	8	(3) 1/4" U clamp	2.0 in	x
Uclmp_2	0.62	3.11	N	8	(2) 1/4" U clamp	1.5 in	x
Cut_2.0in_epx_crimp	1.57	3.11	N	8	steel tube cut	2.0 in	o

Cut_2.5in_epx_crimp	1.99	3.11	N	8	steel tube cut	2.5 in	o
Cut_3.0in_epx_crimp	1.37	3.11	N	8	steel tube cut	3.0 in	o
Split_3	1.31	2.33	N	6	split bolt	2.0 in	x
Split_2_epx	1.99	2.33	N	6	split bolt	2.0 in	o
Split_2_Cut_1in_Epx	3.10	2.33	Y	6	split bolt & steel tube	2.0 in	o
Cut_2in_E	1.68	3.11	N	8	steel tube cut	2.0 in	o
Cut_2.5in_E	0.71	3.11	N	8	steel tube cut	2.5 in	o
Cut_3in_E	1.24	3.11	N	8	steel tube cut	3.0 in	o

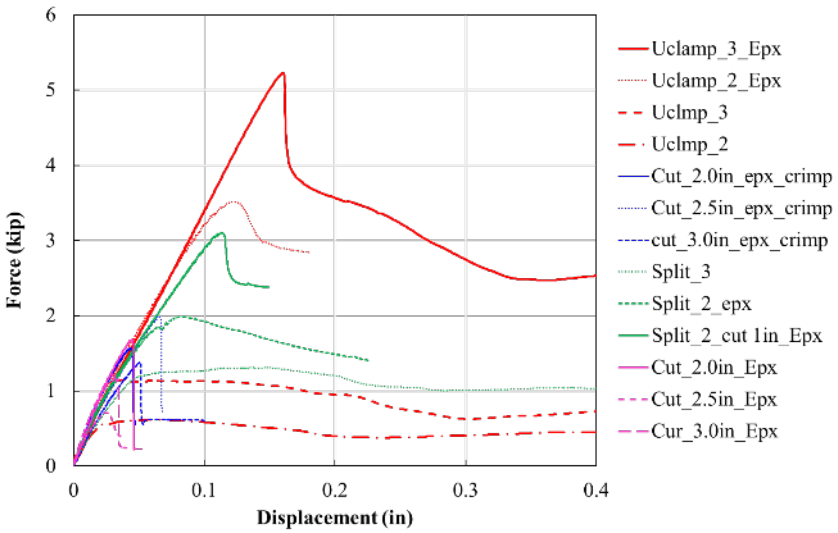

Figure 10 Strength of alternative connection mechanisms

3.2.3. APS design

To verify the feasibility of the APS, a concrete beam specimen with APS was designed and fabricated using connection mechanism developed in previous section. As shown in figure 11a, the size of the concrete beam was 3in by 3in in cross section and 24in long. The APS was located at the centroid of the section. As shown in figure 11b, lengths of zone 1, 2, and 3 were 8in, 8in, and 4in, respectively. The length of the SMA fuse in zone 1 was 5in, thus the length ratio $\left(\frac{A_{steel}}{A_{SMA}}\right)$ was 1.6 (figure 11b). Given that the recovery force generated from the SMA wires was 3.11kips, the nominal prestress level at zone 2 was estimated as 0.345ksi. The concrete mix was designed to meet a target strength of 5ksi at 28 days. Details of assembled APS before casting was shown in figure 12. To provide anchorage, steel wires at zone 3 were bent to 180° to form a hook.

To verify the activation of the wires in zone 1, it was essential to have direct access to the SMA fuse in zone 1. Hence the concrete was cast with a void introduced in zone 1 as shown in Figure 13. The form needed for creating the void was fabricated using 3D printed plastic sleeve. The 3D printed sleeve was placed in the mold during concrete casting. Through the generated void, direct heating of SMA wires was conducted using torch flames (figure 13).

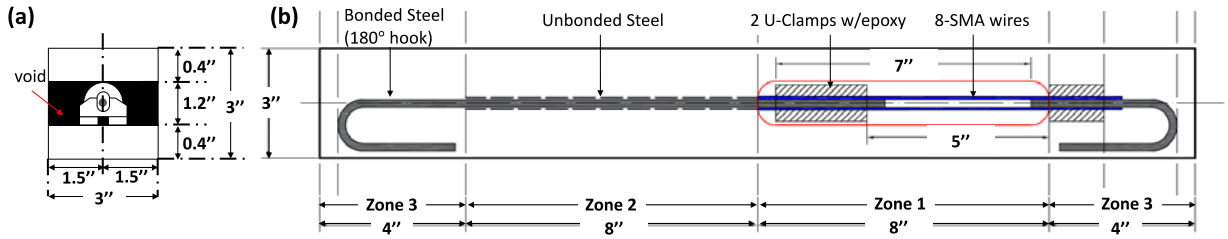

Figure 11 (a) Cross-section at zone 1, (b) elevation view of the APS specimen

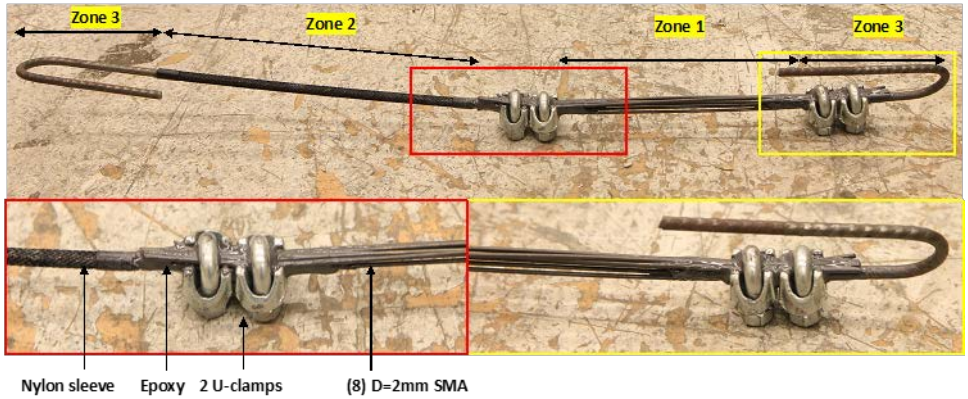

Figure 12 Details of APS

3.2.4. Testing of single APS in concrete beam

Test setup for the activation of the APS window specimen is shown in figure 13. During the activation (heating) of the SMA wires, strain distribution of the front surface of the specimen was measured by DIC cameras located in front of the specimen. Strain at discrete points were measured by the strain gauges attached to the top surface of the middle of zone 1 and zone 2.

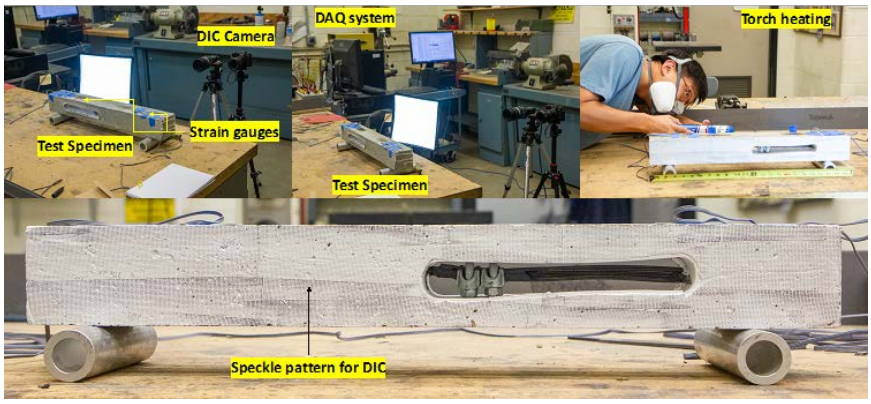

Figure 13 Test setup for APS window

Figure 14 shows comparison of strain distribution from DIC post processed with software Vic2D[2] and FE model using Abaqus[3]. The left side of the leg of the APS fuse was tilted about 5 degrees (figure 14), thus, strain distribution after application of prestress did not indicate perfectly concentric prestress condition. FE model was updated to include the imperfection of the tilted leg of the APS fuse. As shown in the figure, axial strain distribution matched well for DIC and FE model. Center of zone 1 (near the void) showed highest compressive strain concentration and at the end of the specimen showed highest tensile strain concentration. The DIC results showed that the APS fuse can apply prestress to the concrete beam at a target region.

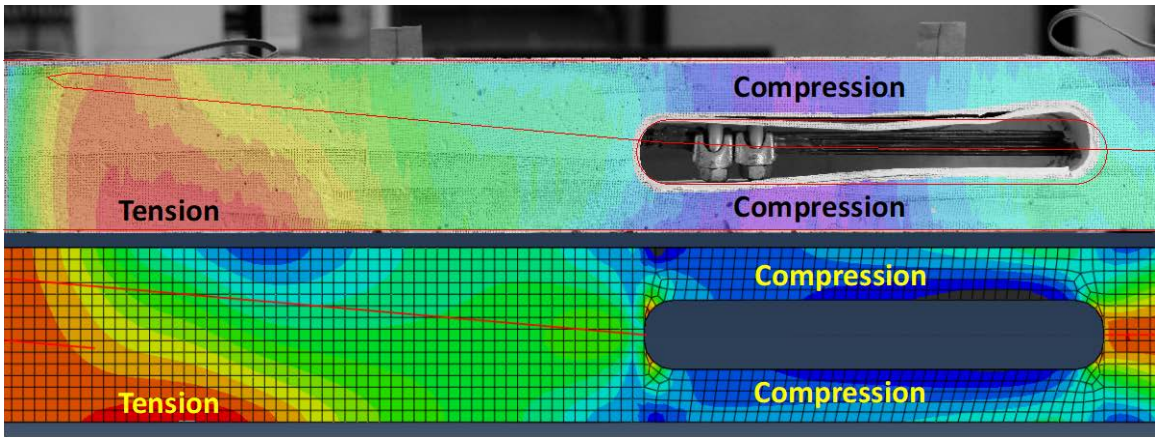

Figure 14 Comparison of axial strain distribution from DIC and FE model prediction

3.3. APS concrete crosstie test

3.3.1. Specimen design

For the last phase of the research, concrete crosstie specimen reinforced with embedded APS was designed and tested. The specimen was designed as ½ scale of the AREMA ch.30[4] based reference tie (figure 15a). The width of the section was 4in. throughout the length and the height was 4in. and 3.2in. at rail seat and center sections respectively, and linearly varying at intermediate zone (figure 15). Figure 15a shows the elevation view of the APS crosstie specimen. Three and two APS assemblies were placed in rail seat and center regions with 1.0in. and 0.6 in. eccentricities, respectively (figure 15b and 15c). At rail seat regions, two 5.3mm diameter low relaxation steel reinforcements were placed with full bond with concrete at 0.75in. from top of the section to provide compressive reinforcement upon loading. Each side of rail seat region was designed to be prestressed by zone 2 of the APS as defined in figure 2a. Center region was also prestressed by zone 2 of the APS, where two SMA fuses were connected to both ends of the zone 2 (figure 15a). Regions near the SMA fuses in zone 1 of the APS were exposed by using voids as explained earlier. Due to the reduced gross area at zone 1, zone 2 was located at the critical locations in rail seat and center region.

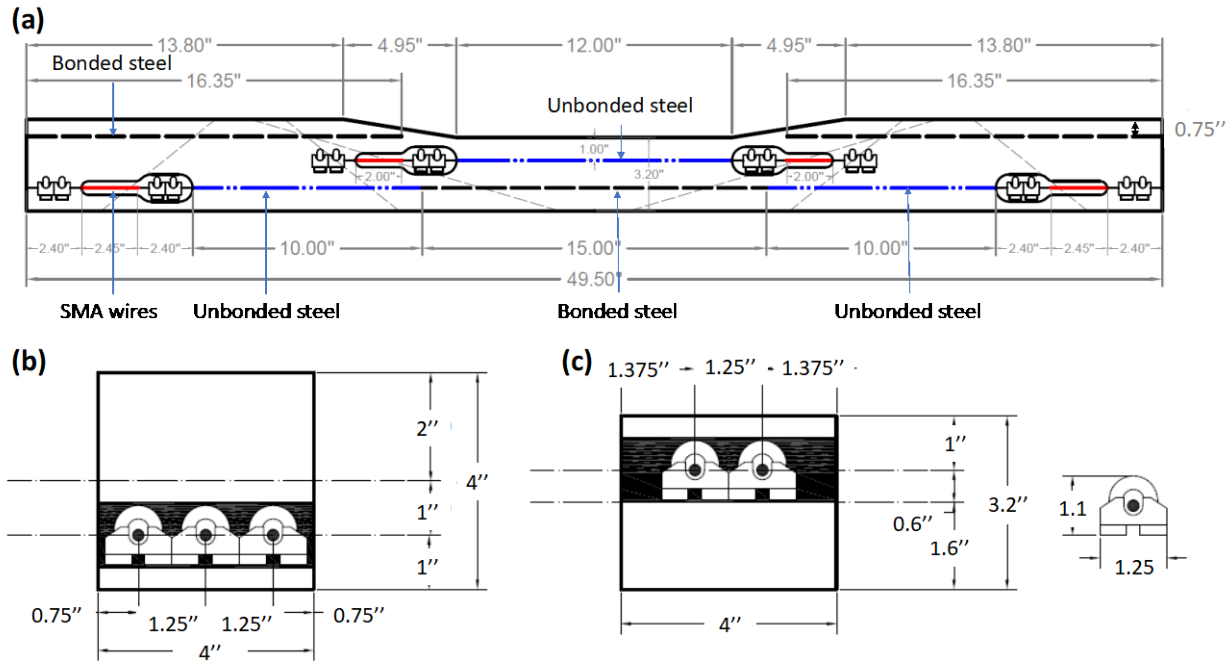

Figure 15 (a) Elevation view of the APS crosstie specimen, (b) rail seat section, (c) center section

As shown in Table 4, area ratio (A_{SMA}/A_{Steel}) of the APS was 1.13 for both rail seat and center regions, whereas the length ratios (L_{SMA}/L_{Steel}) were 0.25 and 0.31 for rail seat and center regions, respectively. According to Eq. 2, the recovery stresses of APS (σ_{SMA}) at rail seat and center regions were 66ksi and 68.4ksi, respectively. At rail seat sections, 1.21ksi of nominal compressive stress was applied at the extreme tensile fiber of the section. This nominal compressive stress at the extreme tensile fiber was 102.79% compared to that of the AREMA ch.30[4] based reference tie. At center section, 1.0ksi of nominal compressive stress was applied at the extreme tensile fiber of the section. This nominal compressive stress was 66.22% of the reference tie.

Table 4 Section design of test specimen

Section	Area ratio	Length ratio	Recovery stress	Prestress at extreme tensile fiber	Percent of equivalent stress at extreme tensile fiber
	A_{SMA}/A_{Steel} -	L_{SMA}/L_{Steel} -	σ_{SMA} (ksi)	σ_{tens} (ksi)	$eqv\ \sigma_{tens}$ (%)
Rail seat	1.13	0.25	66.00	-1.21	102.79
Center	1.13	0.31	68.40	-1.00	66.22

For void regions at zone 1 of the APS, key hole shaped 3D printed sleeve was designed to fit the two U clamps (figure 16). 3D printed sleeves were placed in the mold before casting and were removed after 24h of casting. The void regions were designed to be grouted after the activation of APS. The surface of the 3D printed sleeves were corrugated to avoid the slippage at the interface of the grout and concrete. The design concrete strength was 7ksi at 28 days.

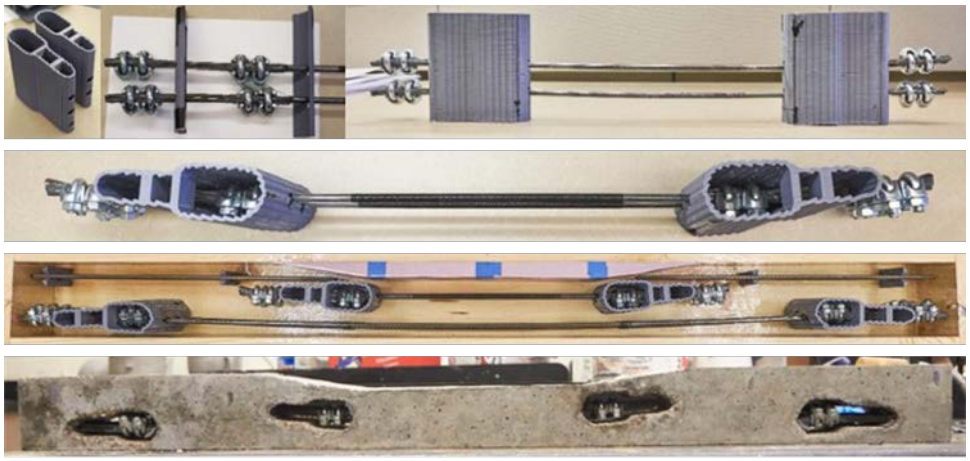

Figure 16 Manufacturing process of the test specimen

3.3.2. Test setup

Two tests were performed with the designed specimen. First, the activation (heating) of APS was performed after 28 days of casting. The specimen was moisture cured for 21 days to reduce creep and shrinkage of the concrete. After 21 days, the specimen was dried and the front surface was covered with a white paint and speckle patterns for DIC. Strain gauges were attached to the top and bottom of the rail seat and center sections (figure 17a). During the activation test, DIC and strain gauges were used to measure the strain distribution of the surface and stain at discrete point of the specimen.

Activation of APS was conducted by heating SMA fuses using propane torch flames through the voids. Heating process was sequentially conducted one region at a time staring with the left rail seat, followed by the right rail seat and then the center section. Each region was heated twice for 10 seconds with one hour of cooling time interval. Rail seat left section (RS_L) was first heated and after two hours of heating and cooling process, rail seat right section (RS_R) was heated, and lastly center section (C) was heated. The detailed test setup of the activation test is shown in figures 17b and 17c.

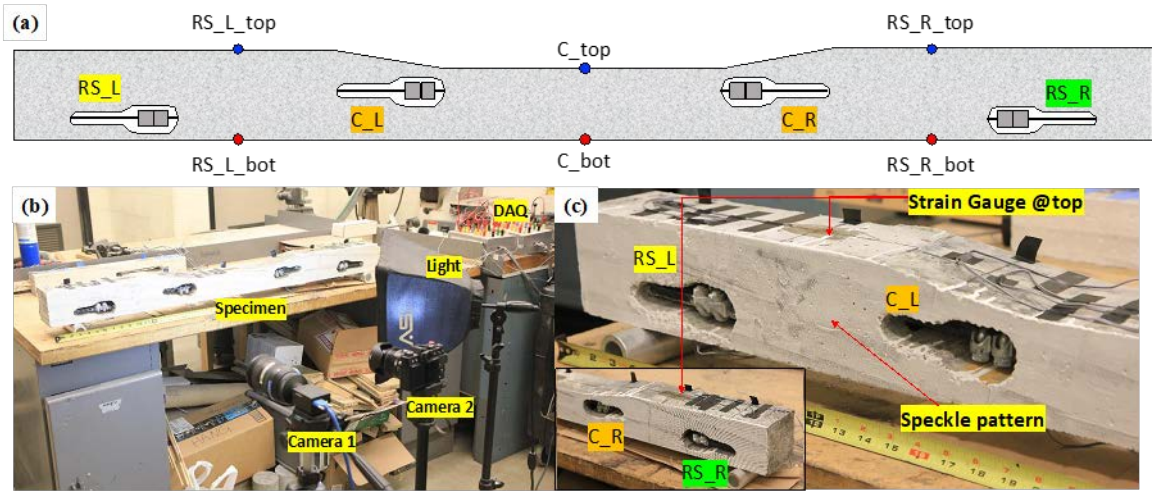

Figure 17 APS activation test setup (a) schematic of sections and location of strain gauges, (b) test setup with specimen and DIC cameras, (c) front side of the rail seat section

Four-point bending tests of the specimen were performed after 30 days of activation of APS and 58 days of casting to examine the strengths at prestressed rail seat and center sections. The bending test was designed as per AREMA ch. 30[4], rail seat positive and center negative bending moment test (figure 18). A day before the bending test, void regions at center and left rail seat were grouted (hatched area in figure 18) with quick set mortar. Right rail seat

section was remained void to compare the effect of grouting. For left rail seat (RS_L) and center (C) sections, load was monotonically applied until failure. For right rail seat section (RS_R), load was monotonically applied until the first crack occurred then the specimen was unloaded. SMA fuse was then re-heated to examine whether it can close the crack. After cooling, RS_R was re-loaded to failure. Four-point bending tests were conducted one region at a time with 20 kip capacity hydraulic loading frame.

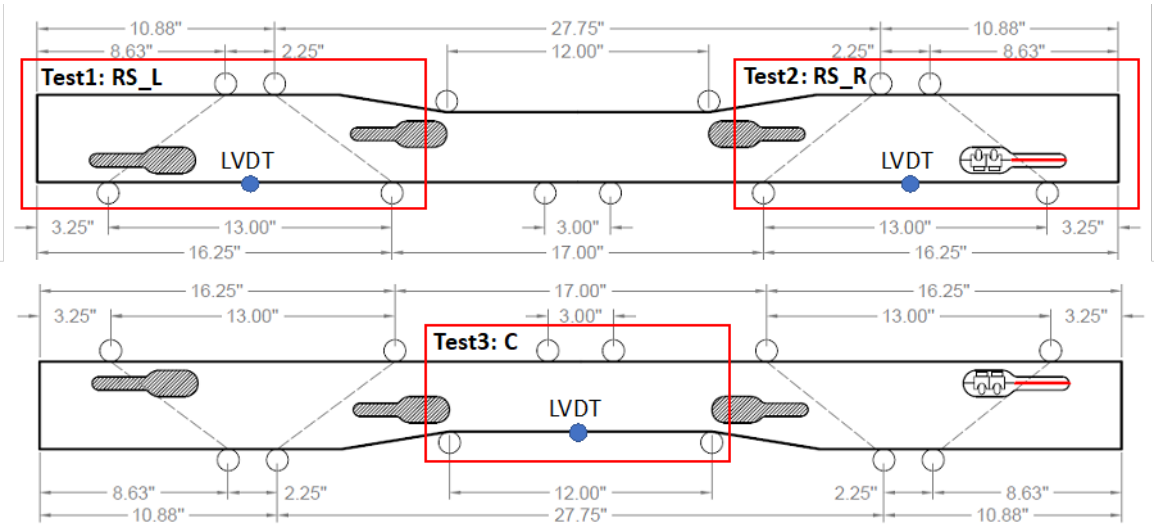

Figure 18 Test setup for loading test (a) rail seat section, (b) center section

3.3.3. Test results

Figure 19a, 19b, and 19c show the time history of strains measured from strain gauges at left rail seat (RS_L), center (C), and right rail seat (RS_R), respectively. RS_L was first heated twice at time 0 min and 60 min and cooled down until 120 min. As shown in figure 19a, bottom strain decreased instantaneously to negative and top strain increased to positive. After the peak, strain level was stabilized to a certain level as the SMA fuse cooled down. This indicated that compressive and tensile strains were applied to the bottom and top of the section.

After 120 min, RS_R was heated twice at time 120 min and 180 min and cooled down until 270 min(figure 19c). As shown in figure 19c, bottom strain decreased instantaneously to negative and top strain increased instantaneously after the application of heat. Strain levels at RS_L and RS_R after 240 min were almost identical to each other. After 270 min, center section (C) was heated twice at 270 min and 330 min. Similar but oppositely, top strain was increased to compressive and the bottom strain was increased to tensile strain right after the application of heat (figure 19b). Figure 19 indicated that the activation of SMA fuse at one section does not affect the strain distribution at other sections. Hence, APS was able to apply local prestressing at the targeted regions independently.

Figure 20 shows a comparison of axial strain distributions from DIC and FE model at RS_L, RS_R, and C. Frames after the activation of each section were selected for post processing the DIC. FE modeling results and DIC strain distributions were plotted with the same color bar scale. Figure 20a, 20b, and 20c indicated a good agreement between DIC result and the FE model. Figure 20a and 20b proved that the compressive strain was applied to the bottom of the rail seat section whereas figure 20c proved that the compressive strain was applied to the top of the center section as designed.

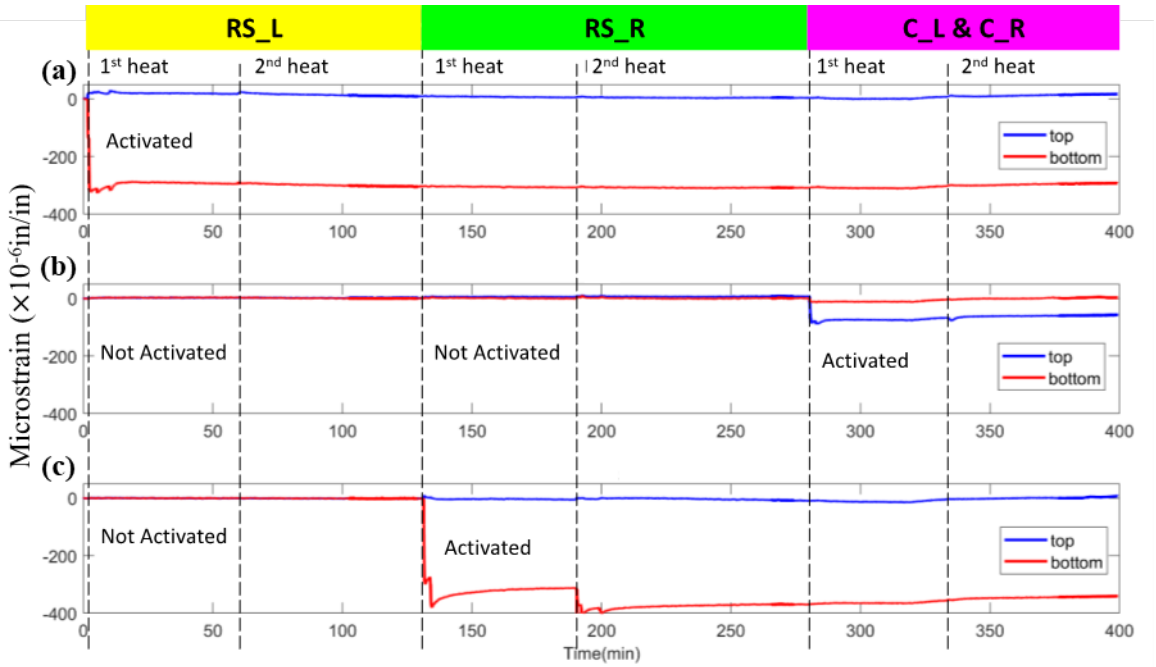

Figure 19 Time history of strains measured from strain gauges at (a) RS_L, (b) C, and (c) RS_R

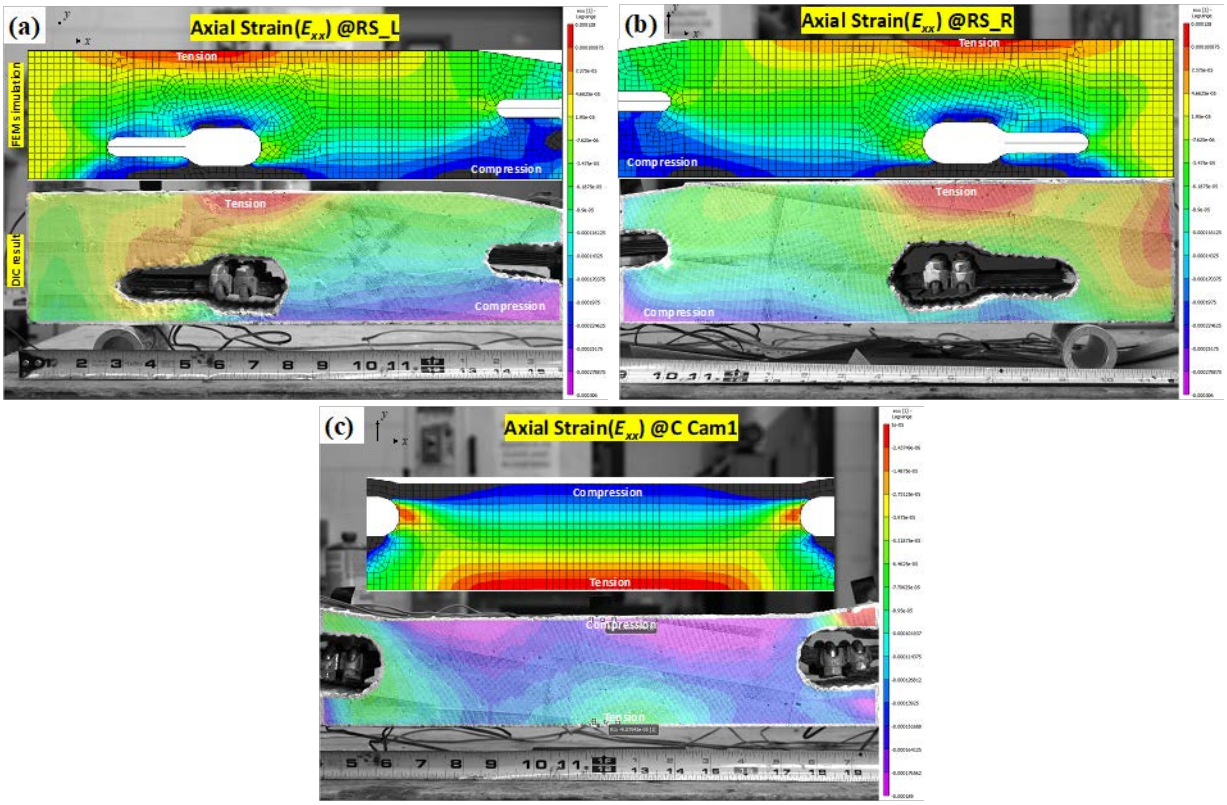

Figure 20 Comparison of axial strain distribution from DIC and FE model at (a) rail seat left (RS_L), (b) rail seat right (RS_R), and (c) center (C)

Figure 21 shows the load versus displacement curve at different sections. Green dash dot line represents the loading curve recorded at RS_L. Black solid line and blue dash line represent the first and reloading curve of RS_R, respectively, and red dotted line represents the loading curve at C. Cracking load of RS_R was observed to be about 4kip, which was closely matching the nominal cracking load of the designed specimen. Both rail seat sections (figure 22a, 22b) failed in shear, whereas the center section failed in flexure. The results of all three sections showed largely ductile post peak behavior because of the use of steel reinforcements at compressive zones. In figure 21, RS_L showed greater cracking and ultimate loads compared to RS_R since the grouting strengthened the void region and improved the load carrying capacity. In figure 22b, void region was excessively deformed upon loading which led to the lower capacity. Corrugated surface at the interface between grout and concrete improved the friction which helped in effectively resisting the deformation of the void region (figure 22a).

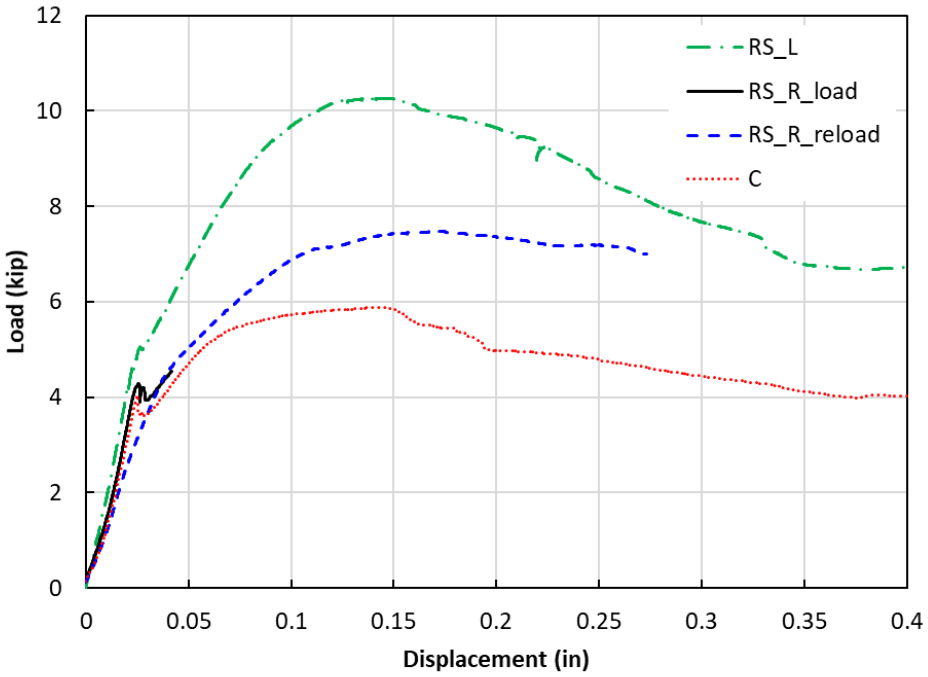

Figure 21 Load vs displacement curve of RS_L, RS_R, and C

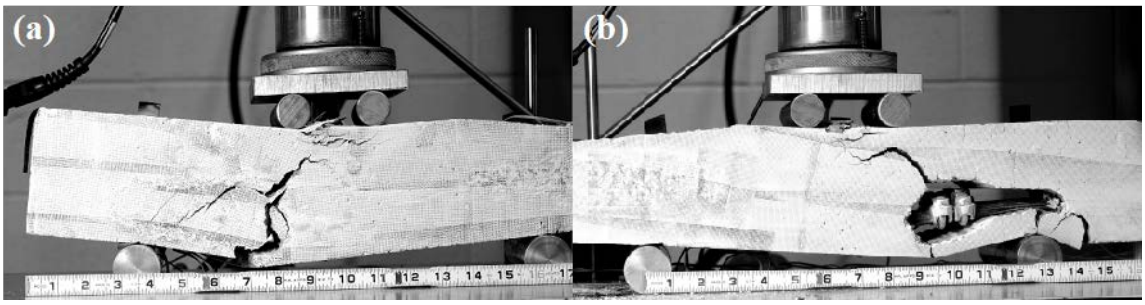

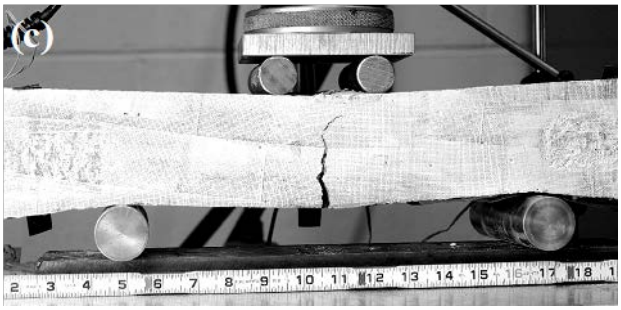

Figure 22 Failure at (a) RS_L, (b) RS_R, (c) C

4. PLANS FOR IMPLEMENTATION

This project proved the concept of using APS for prestressing concrete crossties at target regions where prestressing is required. Although this study proved the advantages of this new technology, there are still several issues that need to be addressed and improved in order for this technology to be implemented successfully. For example, the issue of SMA cost should be addressed through involving SMA manufacturers in investigating the feasibility and cost of SMA mass production. Based on preliminary discussions between the PI and a major SMA manufacturer in the U.S. it was revealed that the price per pound of SMA reduces significantly with the increase of production. For example, producing 300lb of SMA costs only three times the cost of 30lb. Another issue that needs to be investigated is the heating of SMA inside the tie during mass production. One possibility that should be studied is the use of induction heating, which is quite effective in targeting SMA without impacting the surrounding concrete.

To help address these issues, the next step toward implementing this new concept will be to develop and test a prototype of a crosstie prestressed with APS. The prototype should be developed in collaboration with crosstie and SMA producers in the United States. Testing the prototype under realistic loading environment in the lab and the field is essential before this new technology is implemented. Among the features that still need to be improved in the APS are:

• Improving the connection mechanism between SMA fuse and steel to be more seamless through either welding or more efficient mechanical coupling mechanism.
• Studying the use of more cost-effective SMA types (e.g. Fe-based alloys)

5. CONCLUSIONS

A new prestressing system, namely, Adaptive Prestressing System (APS) was proposed and validated in this study. This project focused on three main tasks: (1) Prove the feasibility of applying local prestressing using SMA wires only, (2) Design and fabricate the proposed APS, and (3) Test the proposed APS in a concrete crosstie specimen. To achieve the first task, three small scaled concrete crosstie specimens were designed using SMA reinforcement only. SMA wires were embedded in target regions where prestressing was required. During SMA activation (heating), strain distribution was measured by DIC and strain gauges. The results showed that prestressing force was applied to the targeted regions where SMA was placed.

To achieve the second task of the project, equations were derived to determine the recovery stress of APS using material testing results of SMA specimens. APS was developed with a robust connection mechanism using U clamps and epoxy. The developed APS was then embedded into a prismatic concrete beam for purpose of validation. The activation of APS was verified through monitoring the strains developed in the specimen during heating using DIC and strain gauges. The axial strain distribution from the DIC and FE modeling predictions were compared. The results indicated that the APS was able to apply prestress successfully at the targeted region.

Under the last final task of the project, APS was embedded in a ½-scale concrete crosstie specimen. Two and three APS assemblies were embedded to the center and rail seat regions, respectively. The specimen was designed to have comparable amount of prestress level at the extreme tensile fiber to that of an AREMA-based reference tie. Activation of APS test and four-point bending test were performed. Strains were measured during the activation of

APS by strain gauges and DIC. The comparison of axial strain distribution between DIC and FE model predictions showed a good agreement. Time history of strains at different sections proved that the activation of one section does not affect the other sections of the crosstie. Furthermore, after the activation, test specimen was grouted and loaded to examine its strengths at different sections. The results showed that the cracking load closely matched the design cracking load, and showed largely ductile post-peak behavior. Based on the findings of this Rail Safety IDEA project, it was proven that APS is an innovative technique that holds great promise as a transformative, more efficient, and safer prestressing method for concrete crossties.

6. REFERENCE

1. Otsuka, K., and Wayman, C.M. Shape memory material. *Cambridge University Press*, New edition, 2002.
2. SOLUTIONS, Correlated. Vic-2D. *Reference Manual*, 2009.
3. ABAQUS. ABAQUS user's manual. Version 6.14. 2014.
4. AREMA Manual for Railway Engineering, American Railway Engineering and Maintenance-ofWay Association (AREMA), Landover, Maryland, 2009, v 1, ch. 30